JOURNAL OF AGRICULTURAL AND FOOD CHEMISTRY

J. Agric. Food Chem. **2008,** *56,* 11621–11630 **11621**

Oregano: A Source for Peroxisome Proliferator-Activated Receptor γ Antagonists

MONIKA MUELLER,[†] BRIGITTE LUKAS,[‡] JOHANNES NOVAK,[‡] TOMMASO SIMONCINI,[§] ANDREA RICCARDO GENAZZANI,[§] AND ALOIS JUNGBAUER*,[†]

Christian Doppler Laboratory for Receptor Biotechnology, Department of Biotechnology, University of Natural Resources and Applied Life Sciences, Vienna, Austria, Institute for Applied Botany and Pharmacognosy, University of Veterinary Medicine, Vienna, Austria, and Molecular and Cellular Gynecological Endocrinology Laboratory (MCGEL), Department of Reproductive Medicine and Child Development, Division of Obstetrics and Gynecology, University of Pisa, Pisa, Italy

Peroxisome proliferator-activated receptors (PPARs) are drug targets for several perturbations of metabolic syndrome, defined as the coexistence of obesity, hyperglycemia, hypertension, and hyper/dyslipidemia. In this study, PPAR activation by oregano (e.g., *Origanum vulgare*) and its components was tested. Oregano extracts bind but do not transactivate PPARγ, and binding affinity differs among different oregano extracts. The extracts contain PPARγ antagonists (e.g., quercetin, luteolin, rosmarinic acid, and diosmetin), selective PPARγ modulators (e.g., naringenin and apigenin), and PPARγ agonists (e.g., biochanin A). Oregano extract and isolated compounds in the extract antagonize rosiglitazone-mediated DRIP205/TRAP220 recruitment to PPARγ, pointing to oregano extracts as putative food supplements for weight reduction. Rosmarinic acid and biochanin A, PPARα agonists, may ameliorate the lipid profile. By endothelial nitric oxide synthase activation, oregano extract could prevent atherosclerosis. The results warrant further investigation of oregano extract for its potential to prevent and ameliorate metabolic syndrome and its complications.

KEYWORDS: Metabolic syndrome; *Origanum vulgare*; PPARγ; diabetes; eNOS; rosmarinic acid

INTRODUCTION

Because of the proliferation of a high-calorie, high-fat intake, sedentary lifestyle, obesity has become a worldwide epidemic. It is associated with an increased risk of developing metabolic syndrome, the coexistence of the metabolic perturbations hyperglycemia, hypertension, hyper/dyslipidemia, and central obesity. Cardiovascular morbidity and mortality are more prevalent among patients with this syndrome (*1*).

The peroxisome proliferator-activated receptor (PPAR) isoforms α, γ, and δ are nuclear receptors that play a role in ameliorating the perturbations of metabolic syndrome. After activation, they form a heterodimer with retinoid-X receptors, which can bind to the peroxisome proliferator-response element and promote or decrease the transcription of target genes (*2*). PPARγ is mainly expressed in adipose tissue and has been used as a drug target for treating type 2 diabetes (*2*). Full PPARγ activators, such as the thiazolidinediones currently used for treating type 2 diabetes, have several side effects, including promoting weight gain. Selective PPARγ modulators (SPPARγMs) show antidiabetic action without weight gain because of their mechanism involving only selective cofactor recruitment. Adipogenic cofactors, including DRIP205/TRAP220 and TIF2, are not recruited (*3*). PPARγ antagonists have been shown to exert antiobesity and antidiabetic actions (*4*). The expression of PPARα is mainly in the liver, brown fat, kidney, heart, and skeletal muscle. PPARα activation stimulates the expression of lipoprotein lipase and apolipoprotein A-V, an activator of lipoprotein lipase; it also stimulates the reduction of hepatic apolipoprotein C-III, an inhibitor of lipoprotein lipase, which leads to lower triglyceride levels in chylomicrones and in very low-density lipoprotein particles. Furthermore, PPARα activation leads to an elevated high-density lipoprotein cholesterol level by increased hepatic apolipoprotein A-I and -II expression and to a promotion of cholesterol efflux from cells to high-density lipoprotein by stimulating expression of the ATP-binding cassette A1 transport protein (*2*). PPARδ is ubiquitously expressed. At the cellular level, its activation increases fatty acid oxidation and energy expenditure in the muscles and in adipocytes and lipogenesis in the liver and reduces glucose output in the liver. In vivo, the lipoprotein profile, triglyceride levels, and insulin sensitivity are improved. PPARδ is further suggested to be a drug target in the treatment of obesity (*5*). All three PPAR subtypes play a role in ameliorating athero-

* To whom correspondence should be addressed. Fax: +43-1-3697616. E-mail: alois.jungbauer@boku.ac.at.

[†] University of Natural Resources and Applied Life Sciences Vienna.

[‡] University of Veterinary Medicine Vienna.

[§] University of Pisa.

10.1021/jf802298w CCC: $40.75
Published on Web 11/20/2008

sclerotic status primarily via inhibition of inflammation (*2, 5*). Another mechanism for improving atherosclerosis is activation of endothelial-derived nitric oxide (NO) by ameliorating endothelial dysfunction (*6*).

Natural ligands of the PPARs are fatty acids and their derivatives, such as eicosanoids. The synthetic ligands comprise the group of thiazolidinediones for PPARγ, fibrates for PPARα (*2*), and GW501516 or L-165041 for PPARδ (*5*).

To best of our knowledge, until now, oregano (e.g., *Origanum vulgare*) has not been described as a PPAR ligand, but the hypoglycemic, hypotensive, and hypolipidemic activities of oregano extracts and its compounds have been reported. Oregano and rosmarinic acid, a main phenolic compound, inhibit pancreatic amylase and α-glucosidase, and the components caffeic acid, rosmarinic acid, protocatechuic acid, quercetin, luteolin, and luteolin 7-*O*-glucoside inhibit α-glucosidase (*7*−*10*). Inhibition of both enzymes causes a decrease in the absorption of carbohydrates, resulting in a slower and lower rise in blood glucose. The oregano compounds caffeic acid, chlorogenic acid, and rosmarinic acid also have been reported to decrease glucose production in rat hepatocytes, by an inferred mechanism of induced glucokinase mRNA expression (*11*). Management of hypertension could arise from angiotensin I-converting enzyme inhibition by oregano extract (*9*). Salvianolic acid B has been further reported to have a hypotensive effect because of angiotensin I-converting enzyme inhibitory properties (*12*). In this study, various oregano extracts were examined as potential sources of PPARγ, -α, and -δ ligands or activators.

MATERIALS AND METHODS

Reagents. Solvents, dimethylsulfoxide (DMSO), formic acid, trifluoroacetic acid, apigenin, arbutin, biochanin A, carvacrol, β-caryophellene, *p*-coumaric acid, *p*-cymene, diosmetin, diosmin, eriodictyol, α-humulene, hyperoside, isoquercetrin, isovitexin, limonene, linalool, kaempferol, luteolin, naringenin, naringin, ocimene, peonidin chloride, protocatechuic acid, quercetin, rosmarinic acid, rutin, taxifolin, thymol, ursolic acid, vanillic acid, and vitexin were obtained from Sigma-Aldrich (St. Louis, MO). Salvianolic acid B was purchased from Chromadex Inc. (Santa Ana, CA), and chrysoeriol was purchased from Roth (Karlsruhe, Germany). Rosiglitazone, WY14643, and GW501516 were purchased from Cayman Chemicals (Ann Arbor, MI). Oregano dried leaves, powder, or plant extracts were purchased from different suppliers such as Fuchs (Dissen, Germany), Kotany (Wolkersdorf, Austria), Galke (Gittelde, Germany), Exxentia (Madrid, Spain), Naturex (Avignon, France), Hamburger Gewürzmühle (Hamburg, Germany), Paul Bruns GmbH (Hamburg, Germany), McCormick (United States), Edora (Kleinostheim, Germany), Vivatis Pharma (Hamburg, Germany), Pharmalink (Leichlingen, Germany), Los Chileros de Nuevo Mexico (Santa Fe, NM), Geelawson (London, Great Britain), and Pfannenschmidt (Hamburg, Germany). The black U96 microwell plate was obtained from Nunc (Roskilde, Denmark). The Polar Screen PPARγ Competitive Assay was purchased from Invitrogen Corp. (Carlsbad, CA).

The following were obtained from the stated suppliers: Dulbecco's minimum essential medium (DMEM) for the transactivation assay from Biochrom (Berlin, Germany), fetal calf serum (FCS) from HyClone (Logan, UT), SuperFect from Qiagen (Germantown, MD), and the Dual Glo Luciferase Assay System from Promega (Madison, WI). Acidic ion-exchange resin Dowex 50 W, 200−400 mesh, was purchased from Sigma. 1.1x ReddyMix PCR Master Mix (2.5 mM $MgCl_2$) was purchased from ABgene (Surrey, United Kingdom), primers were obtained from Invitrogen (Lofer, Austria), EXO1 and SAP were purchased from Fermentas (St. Leon-Rot, Germany), and BigDye 3.1 Terminators were obtained from Applied Biosystems (Applera Austria Handels GmbH, Brunn am Gebirge, Austria).

Identification of Plant Materials. Morphological analyses were performed for all samples of small-cut plant material by assessment of calyx morphology. A representative amount of calyces was compared with calyx figures provided in the current taxonomic reference for the genus (*13*) and with calyces of reference herbarium specimens kept at the Institute for Applied Botany and Pharmacognosy (University of Veterinary Medicine, Vienna, Austria).

DNA Analyses. Sequence analyses were performed for all samples included in the study. DNA was extracted from a representative amount of ground leaves, powders, or dried extracts using a modified CTAB extraction following the protocol described in ref *14*. For DNA amplification, two different procedures were used for the different plant preparations. For the fine-cut plant materials and the powders, the nuclear ITS (internal transcribed spacer) region and a part of the nuclear DXS (1-deoxy-D-xylulose 5-phosphate synthase) gene were amplified using universal primers for ITS (ITS5, 5′-GGAAGGAGAAGTCGTAACAAGG-3′; and ITS4, 5′-TCCTTCCGCTTATTGATATGC-3′) (*15, 16*) and EST-derived primers for DXS (DXS24F1, 5′-GGAAGCAAGGTGGCGATTC-3′; and DXS390R1, 5′-GAAACAACAGTCCCTGCGATATG-3′) (*17*). The amplifications were performed on a GeneAmp PCR System 9700 (Applied Biosystems) in 20 μL volumes with the following reaction components: 0.5 μL of template DNA (1−50 ng), 18 μL of 1.1x ReddyMix PCR Master Mix (2.5 mM $MgCl_2$), 0.5 μL of DMSO, 0.2 μL of ddH_20, and 0.4 μL (400 nM) of each primer. For ITS, 35 cycles of amplification with 1 min at 95 °C, 1 min at 55 °C, and 1 min at 72 °C were preceded by a 3 min denaturation step at 95 °C and followed by an additional 7 min at 72 °C. For DXS, 35 cycles of amplification with 1 min at 95 °C, 1 min at 60 °C, and 1 min at 72 °C were preceded by a 3 min denaturation step at 95 °C and followed by an additional 7 min at 72 °C.

Because of the low amounts of extractable DNA for the dried extracts, a nested polymerase chain reaction (PCR) approach for sequence analyses of the ITS region was chosen. In a first PCR, the primers 1406F (5′-TGTACACACCGCCCGT-3′) and 307R (5′-TTGGGCTGCATTCCCA-3′) (*18*) were used as external primers. The amplifications were performed in 15 μL volumes with the following reaction components: 0.5 μL of template DNA (original DNA extract diluted 1:10 with ddH_2O), 13 μL of 1.1x ReddyMix PCR Master Mix (2.5 mM $MgCl_2$), 0.75 μL of DMSO, 0.15 μL of ddH_20, and 0.3 μL (400 nM) of each primer (35 cycles of amplification with 1 min at 94 °C, 1 min at 58 °C, and 2 min at 72 °C, preceded by a 3 min denaturation step at 94 °C and followed by an additional 7 min at 72 °C). The amplification products of the first PCR were cleaned with EXO1 and SAP according to the supplier's instructions and then diluted 1:500 with ddH_2O. A second PCR reaction was carried out with 0.5 μL of this dilution (instead of genomic DNA) with primers ITS4 and ITS5 as nested primers. The PCR conditions were the same as described above.

For sequence analyses, all PCR products were checked on 1.4% agarose gels before being cleaned with EXO1 and SAP. Cycle sequencing was performed in forward and reverse reactions using BigDye 3.1 Terminators and primers from the original amplifications. The sequences were generated with an Applied Biosystems 3130x automated sequencer and edited using Chromas Vers. 2.24 (Technelyseum, Tewantin, Australia).

Because of the small amounts of plant material in the dried extracts, DNA extraction from such plant preparations was sensitive to contamination. Therefore, these samples were extracted and sequenced in duplicate to allow a validation of the results. Blank samples (respectively, nontemplate controls) were included in each extraction procedure and PCR to ensure that no laboratory contamination had occurred.

For identification of the plant samples, an alignment of the sample sequences and reference sequences from a broad range of *Origanum* species and one *Lippia* species (*17*) was conducted with Mega 4 (*19*). Species identification was done on the basis of percent homology with the reference sequences. All sequences have been deposited in GenBank, and accession numbers are listed in **Table 1**.

Extraction and Preparation of the Plants/Plant Powders. A total of 100 mg dry powder of oregano dried leaves or extract were suspended in 1 mL of DMSO for 24 h at room temperature. The suspension was stirred on a magnetic stirrer. After 24 h, the suspension was clarified by centrifugation for 1 h at 13000 rpm. The clear supernatant was used for further analysis.

Table 1. Tested Oregano Materials, Country of Origin, Species According to Supplier Specifications and as Determined by Morphological and DNA Analysis (ITS and/or DXS Gene), the IC_{50} and Equivalent Rosiglitazone Concentration Values of the Oregano Extracts as Determined by the Competitive PPARγ Ligand Binding Assay (LBA), IC_{50} Value and the Equivalent GW9662 Concentration of the Extracts as Determined by PPARγ TR-FRET Antagonist Screening and the Results of GAL4-PPARα, -β, and -γ Transfection Assays

			species (DNA analysis)			PPARγ LBA		TR-FRET	
no.	plant/extract/ standardization	species (acc. to supplier)	species (microscopic analysis)	ITS gene	DOXYP gene	country	IC_{50} (μg/mL)	eq IC_{50} (nmol/g)	IC_{50} (μg/mL)	eq IC_{50} (nmol/g)
1	leaves	*O. onites*	*O. onites*	*O. onites*	*O. onites*	Turkey	1.6 ± 0.3	75025	6.2 ± 0.7	1737
2	leaves	*O. onites*	*O. onites*	*O. onites*	*O. onites*	Turkey	1.8 ± 0.3	66202	2.2 ± 0.2	4910
3	leaves		*O. vulgare*	*O. vulgare*	*O. vulgare*	Albany, Turkey, Greece	3.4 ± 1.3	35057	17.8 ± 1.7	606
4	leaves	*O. onites*	*O. onites*	*O. onites*	*O. onites*	Turkey	3.4 ± 0.3	35805	1.4 ± 0.4	7937
5	extract, >1% rosmarinic acid	*O. vulgare*		*O. majorana*[a]	ND	China	5.3 ± 0.7	22483	2.0 ± 0.2	5395
6	extract 5:1	*O. vulgare*		ND	ND	China	6.8 ± 0.9	17553	2.1 ± 0.4	5035
7	flower					Austria	10.9 ± 1.2	10982		
8	extract 10:1	*O. vulgare*		ND	ND	China	14.0 ± 1.3	8550	23.5 ± 3.9	460
9	leaves	*O. vulgare*		*O. onites*	*O. onites*	Turkey	15.1 ± 3.6	7931	88.7 ± 36.3	121
10	extract 5:1	*O. vulgare*		*O. onites*	ND	China	16.8 ± 2.0	7149		
11	extract 5:1	*O. vulgare*		ND	ND	China	16.9 ± 2.5	7117		
12	extract, >2.5% rosmarinic acid	*O. vulgare*		ND	ND	Bulgaria	20.8 ± 2.6	5771		
13	extract 15:1	*O. vulgare*		ND	ND	China	22.1 ± 1.7	5423	11.9 ± 1.5	903
14	extract 20:1	*O. vulgare*		ND	ND	Spain	23.6 ± 3.3	5081	10.5 ± 1.6	1025
15	extract 10:1	*O. vulgare*		ND	ND	China	27.8 ± 3.5	4314		
16	leaves	*O. vulgare*	O. vulgare	*O. vulgare*	*O. vulgare*		28.6 ± 4.3	4202		
17	leaves	*O. vulgare*	O. vulgare	*O. vulgare*	*O. vulgare*	Albany, Turkey, Greece	29.2 ± 3.9	4010		
18	leaves		*O. vulgare*	*O. vulgare*	*O. vulgare*	Albany, Turkey, Greece	23.6 ± 2.5	5076		
19	extract 15:1	*O. vulgare*		*O. onites*	ND	Spain	32.8 ± 6.9	3664		
20	extract 20:1	*O. vulgare*				Spain	35.3 ± 6.9	3399		
21	leaves	*O. onites*		ND	*O. onites*	Turkey	35.5 ± 4.1	2940		
22	leaves	*O. onites*	*O. onites*	*O. onites*	*O. onites*	Turkey	41.5 ± 8.3	2890		
23	leaves		*O. vulgare*	*O. vulgare*	*O. vulgare*	Spain	41.7 ± 9.2	2874		
24	extract	*O. vulgare*		*O. onites*	ND	Turkey	49.9 ± 3.8	2403		
25	leaves			*Lippia graveolens*	ND	Mexico	52.9 ± 4.6	2270		
26	extract 4:1			*O. onites*	ND		57.0 ± 13.0	2106		
27	extract	*O. vulgare*		*O. onites*	ND	Turkey	65.7 ± 10.0	1826		
28	extract 15:1	*O. vulgare*		ND	ND	China	66.3 ± 134.9	1809		
29	extract	*O. vulgare*		ND	ND	Bulgaria	66.9 ± 6.7	1793		
30	extract			*O. onites*	ND	Turkey	70.2 ± 25.0	1709		
31	extract, >1% rosmarinic acid	*O. vulgare*		ND	ND	Balkans	75.0 ± 7.5	1600		
32	leaves			ND	ND		76.9 ± 7.7	1561		
33	extract 15:1	*O. vulgare*		ND	ND		95.5 ± 23.4	1256		
34	leaves		ND	ND	ND	Austria	100 ± 10.6	1199		
35	extract 4:1	*O. vulgare*		*O. onites*	ND	China	134.1 ± 16.4	895		
36	extract, >1% rosmarinic acid			ND	ND	Turkey	330 ± 71	364		
37	extract 4:1	*O. vulgare*		*O. onites*	ND	China	388 ± 72	309		
38	extract 5:1	*O. vulgare*		ND	ND	Spain	ligand			

[a] Putative hybrids of *O. vulgare* with one species of the *Origanum* section Majorana. ND, not determinable.

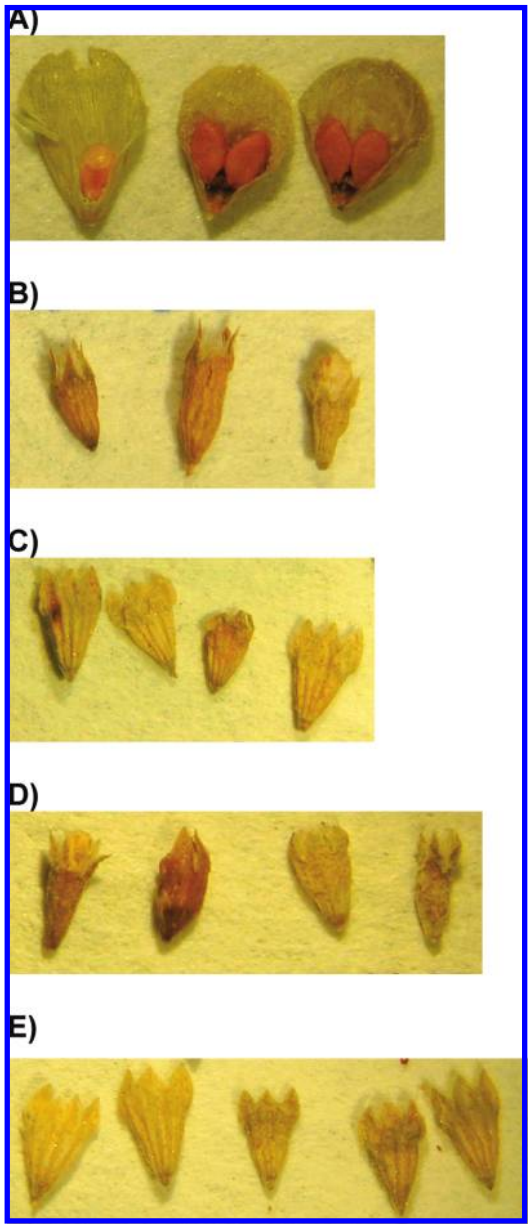

Figure 1. Examples of calyces isolated from *Origanum* small-cut plant materials [(**A**) *O. onites* and (**B**−**E**) *O. vulgare*]. (**A**) Extract 1, (**B**) extract 3, (**C**) extract 16, (**D**) extract 18, and (**E**) extract 23.

Polar Screen PPAR Competitive Assay. A ligand-binding competitive assay was performed using PolarScreen PPARγ Competitor Assay, Green, according to the manufacturer's protocol. Briefly, the PPARγ ligand binding domain (LBD) and the fluorescent PPARγ ligand (Fluoromone PPARγ Green) were combined to form a PPARγ-LBD/fluoromone PPARγ Green complex with a high polarization value. Test compounds in various concentrations competed for binding to PPARγ. Ligands displaced the fluorescent ligand, releasing the fluoromone into the solution to tumble rapidly during its fluorescence lifetime, causing a low polarization value. If substances did not bind to PPARγ and displace the fluorescent ligand from the complex, the polarization value remained high. The change in polarization value was used to determine the relative affinity of test compounds for the PPARγ-LBD. Fluorescence polarization measurements were obtained using a Genios Pro plate reader (Tecan, Crailsheim, Germany) at an excitation wavelength of 485 nm and an emission wavelength of 535 nm. The PPARγ agonist rosiglitazone was used as the standard. The maximal polarization value of rosiglitazone was defined as 100%.

Time-Resolved Fluorescence Resonance Energy Transfer (TR-FRET) Coactivator Assay. Antagonist screening was performed with the Lantha Screen TR-FRET PPARγ coactivator assay in antagonist mode according to the manufacturer's protocol. In brief, different concentrations of various test compounds, the PPARγ LBD tagged with glutathione-*S*-transferase (GST), and a mixture of the fluorescein-labeled coactivator peptide, terbium-labeled anti-GST antibody, and rosiglitazone (final concentration, 250 nM) were combined. Binding of an agonist (in this case rosiglitazone) to PPARγ resulted in a conformational change and coactivator peptide TRAP220/DRIP-2 recruitment. If the fluorescently labeled coactivator peptide and the terbium-labeled anti-GST antibody bound to the PPARγ GST tag came into close proximity, energy was transferred from the terbium label to the fluorescein label, which was detected as emission at 520 nm. Certain concentrations of PPARγ antagonists displaced rosiglitazone from PPARγ, and the emission signal at 520 nm decreased. The fluorescence intensity was measured using the Genios Pro plate reader at an excitation wavelength of 340 nm, emission wavelengths of 520 and 495 nm, a delay time of 100 μs, and an integration time of 200 μs. The emission ratio 520:495 nm was determined. This value indicated the extent of coactivator splitting from PPARγ and thus the antagonistic activity of the substances.

Plasmids. The pGAL4-hPPARγ-LBD, the pGAL4-hPPARα-LBD, and the pGAL4-hPPARδ-LBD expression plasmids, which express chimeric proteins containing the GAL4 DNA binding domain fused to the human PPAR LBD (*20*), was provided by Prof. Staels (Institut Pasteur, University of Lille, France). The luciferase reporter plasmid pFR-Luc containing a firefly luciferase gene controlled by five repeats of GAL4-binding element was purchased from Stratagene (La Jolla, CA). The Renilla control plasmid (pRL-tk), which encodes *Renilla* luciferase, was obtained from Promega.

Transactivation Assay. One day before transfection, NIH-3T3 cells (German Collection of Microorganisms and Cell Cultures, Accession. No. 59) were seeded at a density of 1×10^4 cells per well. Cells were cotransfected with 30 ng of pGAL4-hPPARγ-LBD, 60 ng of pGAL4-hPPARα-LBD, or 30 ng of pGAL4-hPPARδ-LBD expression plasmid, 300 ng of pFR-Luc reporter plasmid, and 15 ng of pRL-TK using the SuperFect transfection reagent. After transfection, the medium was changed, and cells were incubated with standard or test substances dissolved in DMSO for 24 h. The DMSO content of the DMEM did not exceed 0.3%. Luciferase assays were performed using the Dual Glo Luciferase Assay System (following the manufacturer's manual). Firefly luminescence correlating to transactivation efficiency and Renilla luminescence indicating transfection efficiency were measured with the Genios Pro plate reader in luminescence mode. The firefly-to-Renilla ratio was calculated and normalized to the DMSO control. Rosiglitazone (PPARγ agonist), WY14643 (PPARα agonist), and GW501516 (PPARδ agonist) were used as positive controls. The efficiency of these substances was defined as 100%.

Curve Fitting. Data for binding affinity, transactivational activity, and antagonistic activity were processed in the following way: Relative polarization values, transactivational efficiencies, and emission ratio (referred to the reference substance) were plotted against the concentration of test compounds. Curve fitting was performed using a logistic dose−response model (eq 1) of the software Table Curve 2D software (Jandel Scientific, Erkrath, Germany), a nonlinear equation using a Levenberg−Marquard algorithm (*21*).

$$y = a + \frac{b}{1 + (c/x)^d} \quad (1)$$

where a equals the baseline, b is the difference between the plateau of the curve and the baseline, and c is the transition center of the curve, which is the concentration that causes 50% efficiency (ligand potency). d is the transition zone and is a measure of positive or negative cooperativity.

The concentration of the test compounds that results in a half-maximal decrease of polarization value, half-maximal transactivational efficiency, or half-maximal decrease of emission ratio is the IC_{50}/EC_{50} value of the test compound. This value indicates PPARγ binding affinity, transactivational activity, or antagonistic activity.

Statistics. The competitive assay was performed in duplicate, the transactivation assay was performed in quadruplicate, and the TR-FRET

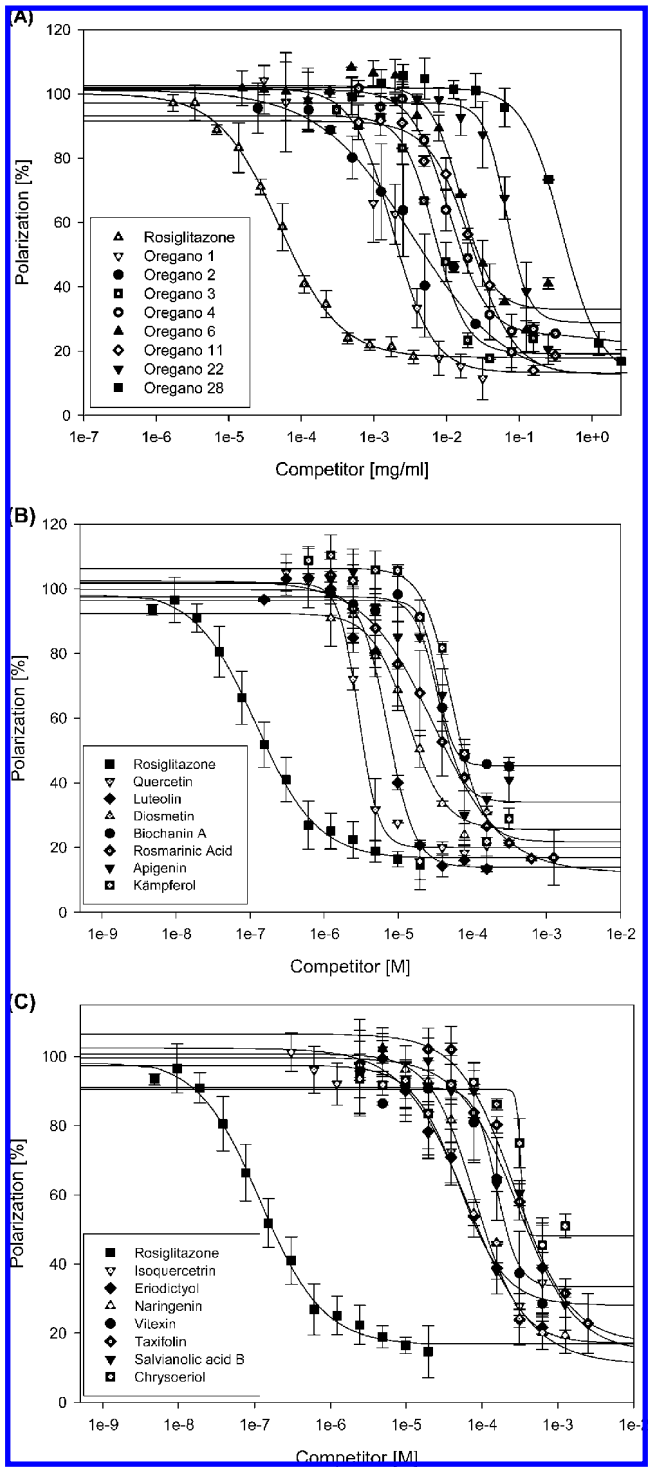

Figure 2. (**A**) Logistic dose−response curves for various oregano extracts, determined using the polar screen PPARγ competitive assay; (**B**) curves for rosiglitazone (standard), quercetin, luteolin, rosmarinic acid, diosmetin, biochanin A, apigenin, and kämpferol; and (**C**) curves for rosiglitazone (standard), isoquercetrin, eriodictyol, naringenin, vitexin, salvianolic acid B, and chrysoeriol.

PPARγ coactivator assay was performed in triplicate. Each assay was performed on independent days, and intervariation was in the same range as intravariation.

Determination of Equivalent Rosiglitazone Concentration. The equivalent rosiglitazone concentration corresponds to the theoretical concentration of rosiglitazone in the extract resulting in the same binding affinity. Rosiglitazone was used as the reference substance. The equivalent IC_{50} value was calculated by dividing the IC_{50} value of rosiglitazone by the IC_{50} value of the plant extracts or isoflavones (eq 2):

$$IC_{50}\,(\text{nmol/g}) = \frac{IC_{50(\text{rosiglitazone})}\,(\text{nmol/L})}{IC_{50(\text{extract})}\,(\text{g/L})} \qquad (2)$$

eNOS Assay: Cell Cultures and Treatments. Human umbilical vein endothelial cells (HUVECs) were harvested enzymatically with type I A collagenase (1 mg/mL), as previously described (*22*), and maintained in phenol red-free DMEM, containing HEPES (25 mM), heparin (50 U/mL), endothelial cell growth factor (50 ng/mL), L-glutamine (2 mM), antibiotics, and 10% FBS. Before each experiment, HUVECs were kept for at least 48 h in DMEM containing 10% steroid-deprived FBS. All experiments were performed on confluent monolayers of endothelial cells. Before every experiment investigating rapid, nontranscriptional effects (up to 30 min treatments), HUVECs were serum starved in DMEM containing no FBS for 8 h before treatment to avoid the confounding effects of serum. Whenever an inhibitor was to be used, we added the compound 30 min before the treatments.

eNOS activity was determined based on the conversion of [^{3}H]arginine to [^{3}H]citrulline in endothelial cell lysates. Converted citrulline was separated by unconverted arginine using the acidic ion-exchange resin Dowex 50 W, 200−400, as described (*23*). Extracts incubated with the eNOS inhibitor, *N*-nitro-L-arginine methyl ester (1 mM), served as the blank.

NO production was determined by a modified nitrite assay using 2,3-diaminonaphtalene, as described (*23*). Fluorescence of 1-(*H*)-naphtotriazole was measured with excitation and emission wavelengths of 365 and 450 nm, respectively. Standard curves were constructed with sodium nitrite. Nonspecific fluorescence was determined in the presence of NG-monomethyl-L-arginine (3 mM).

High-Performance Liquid Chromatography−Electrospray Ionization−Mass Spectrometry (HPLC-ESI-MS) Analysis. Separation for a HPLC-MS was carried out with a Finnigan Surveyor Plus HPLC system (ThermoFinnigan, San Jose, CA) connected with a Luna C18(2) column (3 μm, 100 mm × 2 mm, Phenomenex, Torrance, CA) and a security guard cartridge (Phenomenex). The mobile phase consisted of solvent A (5% acetonitrile, 0.1% formic acid) and solvent B (acetonitrile, 0.1% formic acid). The gradient profile was as follows: from 0−5 min, 100% B; 5−30 min, from 0 to 17.5% A; 30−55 min from 17.5 to 50% A; 55−65 min, 50% A; 65−75 min, 90% A; 75−78 min, 100% B; 78−88 min, 90% A; and 88−90 min, 100% C. Mass analyses were performed with an LTQ ion trap mass spectrometer (ThermoFinnigan) equipped with an electron spray ionization source as previously described (*24*).

RESULTS

Commercial sources of different oregano plant material were purchased. To ensure the identity as oregano and further characterize these materials, morphological and DNA analyses were performed. The results of the morphological and DNA analyses are summarized in **Table 1**. Most of the traded oregano in the "old world" is derived from plant material of the species *O. vulgare* and *Origanum onites* (*25*). Because these two species show very different calyx characteristics, this morphological feature is an appropriate tool for determining samples of small-cut plant material and to distinguish the "Mexican oregano," which derives mainly from *Lippia* sp. (Verbenaceae) (*25*). Out of 38 samples, nine could be analyzed morphologically, and the other samples were extracts. Five samples were identified as *O. vulgare* and four as *O. onites* (**Figure 1**).

The results of the DNA analyses were in accordance with the morphological analyses. Out of 38 analyzed samples, sequences were only obtained with 20 samples. Thirteen were identified as *O. onites*, five as *O. vulgare*, one as *Lippia* sp., and one as *O. majoranum*. The success of sequence analyses was correlated with the particular preparation of the plant

Table 2. IC_{50} Values of Substances Occurring in Oregano, Determined by Competitive PPARγ LBA, the IC_{50} Value of Oregano Compounds Determined by TR-FRET Assay in Antagonist Mode, and the EC_{50} Value and Efficiency (%) of Oregano Compounds, Determined by Chimeric GAL4-PPARγ, GAL4-PPARα, or GAL4-PPARδ Transfection Assay

		PPARγ				PPARα		PPARδ	
		LBA	TR-FRET	transactivation		transactivation		transactivation	
substance	CAS no.	IC_{50} (μM)	IC_{50} (μM)	EC_{50} (μM)	efficiency[d] (%)	EC_{50} (μM)	efficiency (%)	EC_{50} (μM)	efficiency (%)
rosiglitazone	122320-73-4	0.12 ± 0.01		0.21 ± 0.05	100.0				
GW9662	22978-25-2		0.013 ± 0.002						
WY 14643	50892-23-4					10.5 ± 1.4	100.0		
GW 501516	317318-70-0							0.0005 ± 0.0001	100.0
quercetin	849061-97-8	3.0 ± 0.2	3.7 ± 0.4	ND[e]		ND		ND	
luteolin	491-70-3	7.2 ± 0.6	4.9 ± 0.4	ND		ND		ND	
diosmetin	520-34-3	13.5 ± 2.0	antagonist[b]	ND		ND		ND	
biochanin A	491-80-5	23.7 ± 6.2	ND	32.1 ± 6.4	26.5	23.6 ± 2.1	54.7	ND	
rosmarinic acid	20283-92-5	32.4 ± 4.0	43.6 ± 4.2	ND		43.0 ± 5.3	19.4	ND	
apigenin	520-36-5	40.9 ± 9.1	antagonist	active[c]	15.7	ND		ND	
kämpferol	520-18-3	47.6 ± 8.2	32.9 ± 4.0	ND					
isoquercetrin	21637-25-2	49.9 ± 8.8	antagonist	ND		ND		ND	
eriodictyol	552-58-9	66.6 ± 11.9	16.1 ± 8.1	ND		ND		ND	
naringenin	67604-48-2	81.0 ± 10.3	35.3 ± 15.2	79.5 ± 9.0	16.4	ND		ND	
vitexin	3681-93-4	155.7 ± 18.7	30.6 ± 1.4	ND		ND		ND	
taxifolin	480-18-2	275.4 ± 40.4	75.7 ± 41.8						
salvianolic acid B	115939-25-8	ligand[a]	antagonist	ND		ND		ND	
chrysoeriol	491-71-4	ligand	ND	ND					
carvacrol	499-75-2	ligand	antagonist						
naringin	10236-47-2	ligand	ND						
thymol	89-83-8	ligand							
limonene	5989-27-5	ligand							
peonidinCl	134-01-0	ligand							
ursolic acid	77-52-1	ligand							
apigenin-7-glycoside	578-74-5	ligand							
p-coumaric acid	501-98-4	ligand							
vanillic acid	121-34-6	ligand							
isovitexin	29702-25-8	ND							
hyperoside	482-36-0	ND							
arbutin	497-76-7	ND							
protocatechuic acid	99-50-3	ND							
linalool	78-70-6	ND							
β-caryophellene	87-44-5	ND							
ocimene	13877-91-3	ND							
caffeic acid	331-39-5	ND							
diosmin	520-27-4	ND							
p-cymene	99-87-6	ND							
α-humulene	6753-98-6	ND							

[a] Compounds that bound to PPARγ lacking saturation of the logistic dose−response curve were described as ligands. [b] Compounds antagonizing rosiglitazone-mediated coactivator recruitment in the TR-FRET assay without reaching a plateau for the minimum value were described as antagonists. [c] If transactivation was observed (firefly luciferase value ≥1.5-fold the DMSO control), but no EC_{50} value could be determined, compounds were described as active. [d] The efficiency describes the maximal induction referred to rosiglitazone using the chimeric GAL4-PPAR assay. [e] For some substances, no binding or transactivation was observed (ND, not determinable) up to a concentration of 2.5 (LBA) or 0.3 mM (transactivation assay).

materials. DNA extraction from leaves and powders and subsequent sequencing is a standard procedure, and the two different DNA markers used allowed an unambiguous determination of the respective plant material. Because of the tiny amounts of plant residuals and therefore extractable DNA, work with extracts is much more sensitive. Dealing with traces of DNA amplification of the DXS region was not possible; thus, amplification of the ITS region was successful only for some of the dried extract samples (**Table 1**).

The binding affinity of oregano extract and its compounds for PPARγ was determined by a competitive assay based on the ability of the samples to displace the above-described fluorescent PPARγ ligand. Data were approximated by logistic dose−response curves, and potency values were derived. A great variety of oregano extracts was assayed to get a first insight how the PPARγ binding affinity varied with different influences like species, growing area, and climatic influences. The PPARγ affinity of the different samples varied in a wide range from an IC_{50} value of 1.6 ± 0.3 to 500 μg/mL (**Table 1** and **Figure 2A**). At first glance, one cannot conclude that a certain species was a higher PPARγ binder.

Polyphenolic compounds, typically present in oregano, were also tested (*26, 27*). A total of 23 different compounds that bind to the receptor could be identified. The most potent substances where quercetin (IC_{50} = 3.0 μM), luteolin (IC_{50} = 7.2 μM), rosmarinic acid (IC_{50} = 32.4 μM), and diosmetin (IC_{50} = 13 μM) (**Figures 2 B**,**C** and **Table 2**). Some compounds did not bind to PPARγ up to a concentration of 0.025 M: isovitexin, hyperoside, arbutin, protocatechuic acid, linalool, β-caryophellene, ocimene, α-humulene, *p*-cymene, caffeic acid, and diosmin.

For determination of transactivation properties, the extracts were assayed by transfection assay. The transactivation assay was performed by cotransfection of NIH-3T3 cells with pGAL4-hPPARγ-LBD, pGAL4-hPPARα-LBD, or pGAL4-hPPARδ-LBD and a luciferase reporter plasmid. Transiently transfected cells were incubated with substances at a concentration range from 3×10^{-4} to 1×10^{-6} M and plant extracts up to a concentration of 0.3 mg/mL. Logistic dose−response curves

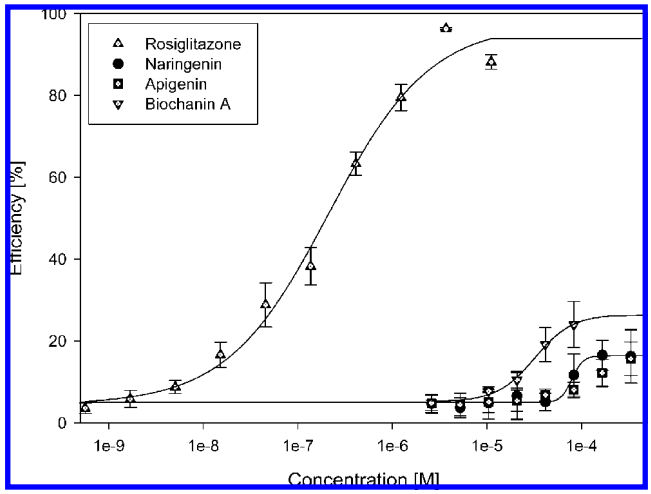

Figure 3. Logistic dose−response curves for rosiglitazone, biochanin A, naringenin, and apigenin, determined by chimeric GAL4-PPARγ transfection assay.

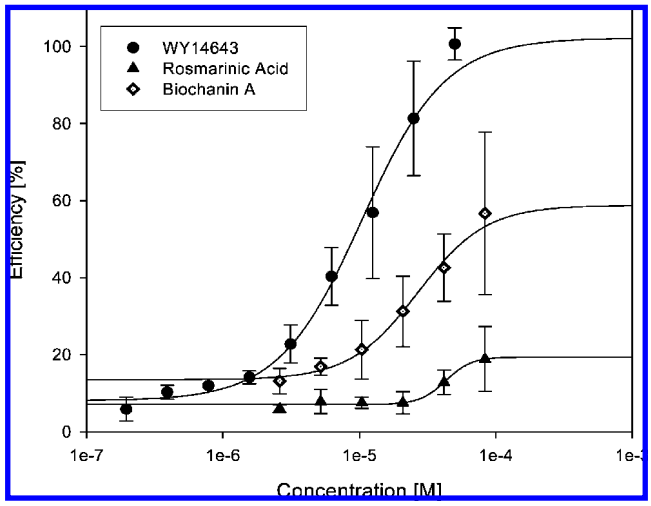

Figure 4. Logistic dose−response curves for WY14643, biochanin A, and rosmarinic acid, determined by chimeric GAL4-PPARα transfection assay.

were calculated as described above, and activity and potencies were derived from the fitted parameters.

The oregano compounds naringenin and apigenin showed moderate PPARγ transactivational activity with respective EC_{50} values of 79.5 and 201.1 μM and a respective maximal activation of 16.4 and 15.7% as compared to rosiglitazone (**Figure 3** and **Table 2**). Biochanin A was a potent PPARγ transactivator (EC_{50} = 32.1 μM; maximal activity of 26.5%). Various oregano extracts and the compounds rosmarinic acid, quercetin, isoquercetrin, vitexin, salvianolic acid B, chrysoeriol luteolin, diosmetin, eriodictyol, and taxifolin did not show PPARγ transactivational activity. Oregano extract and some of the oregano compounds exerted cytotoxic activity. This activity was especially high for luteolin, quercetin, and diosmetin, beginning at a concentration of 10 μM.

For PPARα transactivation assays, WY14643, a known PPARα agonist, served as the control substance (EC_{50} = 10.5). Rosmarinic acid, the main phenolic compound of oregano extract, was a weak transactivator (EC_{50} = 43.0 μM), and biochanin A was a moderate transactivator (EC_{50} = 23.6 μM) (**Figure 4** and **Table 2**). The maximum activity (as compared to the activity of WY14643, defined as 100%) was 19.4% for rosmarinic acid and 54.7% for biochanin A. No significant

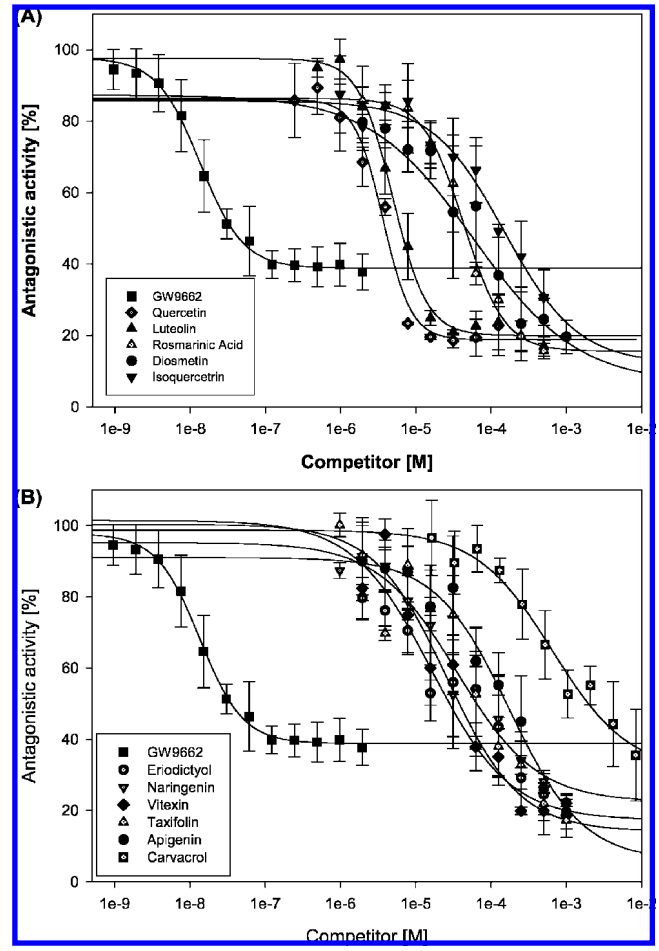

Figure 5. Logistic dose−response curves for (**A**) GW9662, quercetin, luteolin, rosmarinic acid, diosmetin, biochanin A, and isoquercetrin and (**B**) eriodictyol, naringenin, apigenin, vitexin, taxifolin, and carvacrol, determined by the TR-FRET assay in antagonist mode.

transactivational activity was observed for vitexin, naringenin, apigenin, eriodictyol, and isoquercetrin. Luteolin, quercetin, and diosmetin did not activate PPARα but showed high cytotoxic activity. Different oregano extracts and the abundant compound salvianolic acid also did not transactivate PPARα.

Various oregano extracts and the oregano compounds quercetin, luteolin, rosmarinic acid, diosmetin, biochanin A, isoquercetrin, naringenin, eriodictyol, apigenin, vitexin, and salvianolic acid B did not transactivate PPARδ.

With TR-FRET assay, the antagonistic activity of oregano compounds and extracts was analyzed. The reference substance GW9662 antagonized rosiglitazone-mediated TRAP220/DRIP-2 coactivator recruitment with an IC_{50} of about 14 nM. Luteolin (IC_{50} = 4.9 μM), isoquercetrin (IC_{50} = 15.1 μM), quercetin (IC_{50} = 3.7 μM), vitexin (IC_{50} = 30.6 μM), rosmarinic acid (IC_{50} = 43.6 μM), eriodictyol (IC_{50} = 16.1 μM), taxifolin (IC_{50} = 75.7 μM), naringenin (IC_{50} = 35.3 μM), diosmetin, salvianolic acid, apigenin, and carvacrol showed significant antagonistic activity in this assay (**Figure 5** and **Table 2**). The IC_{50} value of the oregano extracts ranged from 1.4 (extract 4) to 88.7 (extract 9, **Table 1**).

Endothelial NO synthase (eNOS) activation is also a good indication for vascular health. This was assayed by exposure of umbilical vein endothelial cells to oregano extract. A concentration-dependent increase in NO release with a maximum of approximately 20-fold induction as compared to negative control in the cell culture medium, which was

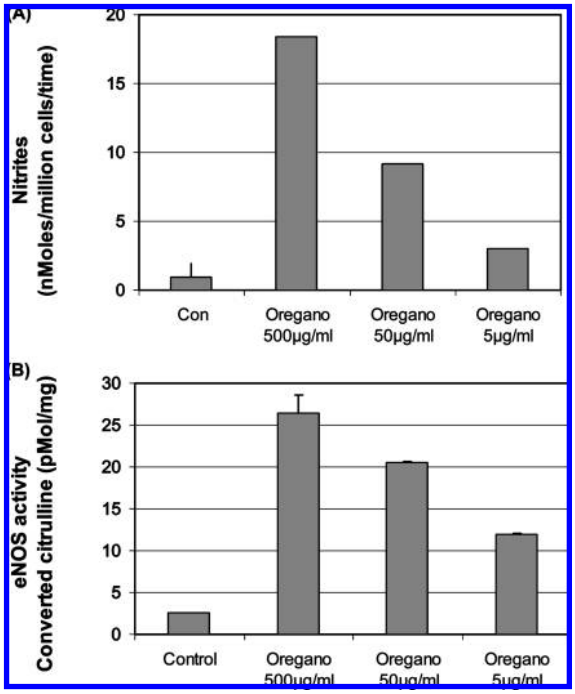

Figure 6. Influence of oregano extract on (**A**) nitrites formation and (**B**) endothelial nitric oxide synthase (eNOS) activity in human endothelial cells.

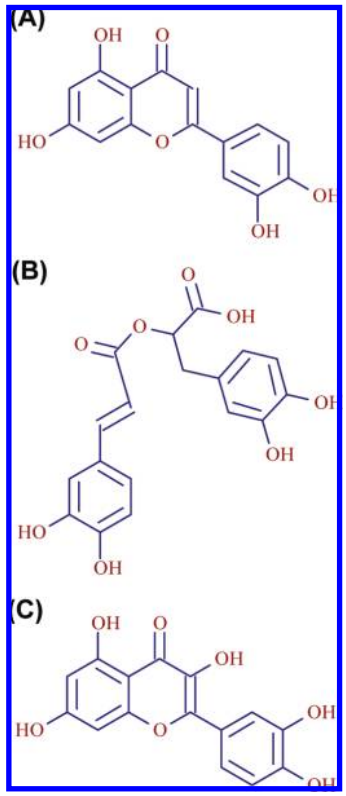

Figure 7. Structures of (**A**) luteolin, (**B**) rosmarinic acid, and (**C**) quercetin.

associated with a parallel activation of eNOS reaching a maximum of approximately 10-fold induction (**Figure 6**), was observed.

To determine the occurrence of compounds in oregano, the extract with the highest PPARγ-binding affinity (extract no. 1) was further analyzed by HPLC-MS. With the use of authentic standards, certain compounds could be identified as rosmarinic

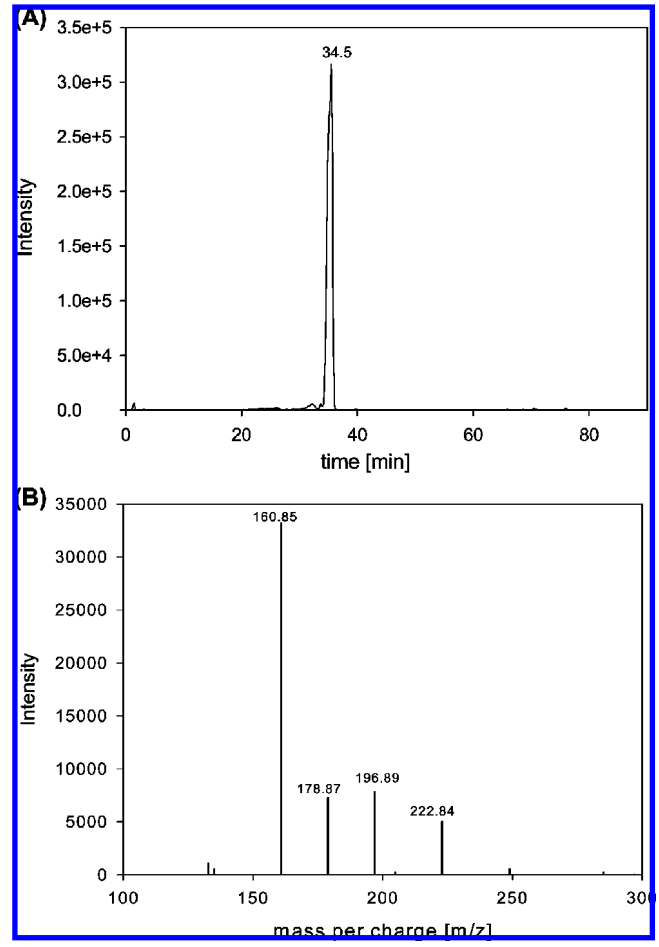

Figure 8. (**A**) MS/MS chromatogram of the mass −1 of rosmarinic acid, 359.3 and (**B**) spectrum of the MS/MS experiment from the precursor mass of 359.0.

Table 3. Retention Time (T_R) and Mass Spectrometry (MS) Data for Standards, Determined by HPLC-MS[a]

substance	T_R (min)	$[M - H]^-$ (*m*/*z*)	fragment ions (*m*/*z*)
quercetin	37.8	301.0	178.8, 150.8, 272.9
rosmarinic acid	31.8	359.0	160.8, 178.8, 196.8, 222.9
luteolin	38.3	285.0	240.9, 198.9, 174.87
biochanin A	53.3	283.1	267.9
isoquercetrin	25.1	463.0	301.9
apigenin	42.1	271.1	224.9, 148.9, 200.1
naringenin	43.1	271.3	150.8, 176.9, 124.9
taxifolin	26.0	303.1	284.9, 176.9, 124.9
apigetrin	32.8	431.2	269.0
chrysoeriol	44.4	299.1	285.1
rutin	27.2	609.1	343.0, 300.9, 270.9
naringin	32.2	579.1	459.0, 270.9, 313.0
kämpferol	44.1	284.9	150.8, 256.9, 240.9
diosmetin	42.0	299.1	283.9
apigenin-7-glycoside	32.8	431.2	268.9
salvianolic acid B	38.9	717.0	518.9, 536.9,321.0
eriodictyol	35.6	287.0	268.9, 242.9, 150.8
diosmin	33.5	607.0	298.9, 283.9

[a] With full MS mode, molecule ions $[M - H]^-$ are derived; in MS/MS mode, fragment patterns are derived, which serves for identification of a specific substance.

acid, quercetin, luteolin, biochanin A, isoquercetrin, apigenin, naringenin, taxifolin, apigetrin, chrysoeriol, rutin, naringin, kämpferol, diosmetin, apigenin-7-glycoside, salvianolic acid B, eriodictyol, and diosmin (**Figures 7** and **8** and **Tables 3** and **4**). Rosmarinic acid was the most abundant phenolic compound in the oregano extract. The MS/MS spectrum of rosmarinic acid (MS-1 = 359.3 g) is shown in **Figure 6** with the most abundant

Table 4. Retention Time (T_R) and MS Data for the Main Compounds Present in *O. onites* (Oregano Extract 1)[a]

T_R (min)	$[M - H]^-$ (*m*/*z*)	fragment ions (*m*/*z*)	compound identified
53.0	283.1	268.0	biochanin A
38.0	301.2	178.8, 150.8, 272.9	quercetin
32.4	359.3	160.8, 178.8, 196.8, 222.9	rosmarinic acid
24.8	463.4	301.9	isoquercetrin
39.0	285.2	240.9, 198.9, 174.87	luteolin
43.0	271.3	150.8, 176.9, 124.9	naringenin
25.9	303.2	284.9, 176.9, 124.9	taxifolin
32.6	431.4	269.0	apigetrin
26.25	299.3	285.1	glycoside of chrysoeriol
27.0	609.5	343.0, 300.9, 270.9	rutin
39.5	717.6	518.9, 536.9,321.0	salvianolic acid B
36.7	287.3	268.9, 242.9, 150.8	eriodictyol
33.6	607.0	298.9, 283.9	diosmin
44.4	284.9	150.8, 256.9, 240.9	kaempferol
42.2	299.1	298.9, 283.9	diosmetin
42.2	271.1	224.9, 148.9, 200.1	apigenin

[a] With full MS, molecule ions $[M - H]^-$ are derived; with MS/MS, fragment patterns are derived, which serves for identification of a specific substance.

peak at a retention time of 34.5 min and the main fragment of 160.85 g. The dimer of rosmarinic acid, salvianolic acid B, was the second most abundant peak. All other compounds occurred only in small amounts.

DISCUSSION

Metabolic syndrome is a multifactorial, severe health problem that affects a large number of people worldwide. This syndrome comprises metabolic risk factors such as abdominal obesity, insulin resistance, hyper/dyslipidemia, and hypertension, a combination that increases the risk for developing cardiovascular disease or type 2 diabetes (*1*). Primary treatment of this syndrome should be a change in lifestyle, including increased physical activity, calorie restriction, and changes in diet. If the cardiovascular risk is too high or the lifestyle changes are not sufficient, medical treatment of the metabolic syndrome is recommended. Treatment of several perturbations of the metabolic syndrome is recommended for reducing cardiovascular risk because the risk factors have a multiplicative impact on cardiovascular risk (*1*).

PPARs have been shown to have a positive effect on the disorders related to metabolic syndrome (*2*). Oregano extract is a putative candidate for treating several aspects of metabolic syndrome, and we found that different oregano extracts are moderate PPARγ ligands. Oregano extract contains mainly PPARγ antagonists such as quercetin, luteolin, rosmarinic acid, and diosmetin, SPPARγMs like naringenin and apigenin, and PPARγ agonists like biochanin A.

Extracts of oregano and almost all associated substances moderately antagonized rosiglitazone-mediated DRIP205/TRAP220 recruitment. This cofactor was recently classified among the so-called "adipogenic factors", indicating that it promotes adipogenesis and adipocyte differentiation in cell culture and thus weight gain in humans. PPARγ antagonists have been suggested to have potential as antiobesity drugs (*3, 4*). Recently, it was shown that insulin resistance is also improved by PPARγ antagonists; because of a lower adipocyte mass, lower levels of adipokines that promote insulin resistance are secreted, thus resulting in a reduced risk of developing diabetes (*4*). Hypoglycemic activity of oregano extract also has been reported, but the proposed mechanism differs. It was proposed that oregano extracts exert hypoglycemic activity through inhibition of pancreatic amylase and α-glucosidase (*7*−*10*).

As mentioned, oregano extract contains the PPARα agonists rosmarinic acid and biochanin A, which might be expected to contribute to an improved lipid profile. However, because the extract did not transactivate the receptor, the agonistic activity of those substances may be too low or oregano may also contain PPARα antagonists that counteract the agonistic activity.

Oregano extracts also have the potential to treat secondary complications of diabetes. Human endothelial cells are central for the function of human vessels in physiological and pathological conditions, and the synthesis of the vasodilatory and anti-inflammatory molecule NO by endothelial cells is of paramount importance for vascular function (*28*). As an activator of eNOS, oregano extract has the potential to improve endothelial dysfunction and thus atherosclerosis (*6*). The oregano compounds quercetin and kaempferol showed inhibitory effects on glucose-induced low-density lipoprotein lipid peroxidation, which helps to prevent arteriosclerosis (*29*).

Currently, diabetes is treated with glitazones like rosiglitazone and pioglitazone, and fibrates are used for treatment of dyslipidemia. Limitations and side effects of these drugs, such as weight gain and edema, have reinforced the need for drugs that ameliorate perturbations of metabolic syndrome without severe side effects (*30*). Oregano extracts represent an interesting alternative for treatment of obesity and metabolic syndrome because of its wide spectrum of health-ameliorating effects, starting with the prevention of obesity and thus of metabolic syndrome, and ameliorating metabolic syndrome and diabetic complications. We showed that it is a candidate for investigation in the treatment of obesity and diabetes via PPARγ antagonism, treatment of hyperlipidemia because it contains PPARα agonists, and the prevention and amelioration of atherosclerosis by eNOS activation. Literature reports showed the hypotensive effect of oregano extracts or its compounds (*9, 12*).

Further studies are required for standardizing oregano extracts for treatment of obesity and related disorders. Species, climate, and growing area seem to have important influences on the synthesis of PPARγ antagonists.

Here, we present only putative effects of oregano extract based on in vitro data. In vivo assays and clinical trials would be necessary to confirm any health-ameliorating effects of oregano extract in humans and to decide which biologic properties contribute to amelioration of metabolic syndrome. It would also be of interest to evaluate whether different mechanisms act together in producing beneficial effects.

In conclusion, oregano extract contains PPARγ antagonists, like quercetin, luteolin, rosmarinic acid, and diosmetin, SPPARγMs like naringenin and apigenin, PPARγ agonists, like biochanin A, and PPARα agonists rosmarinic acid and biochanin A. Rosiglitazone-mediated DRIP205/TRAP220 recruitment is antagonized by oregano extract and nearly all components, which could contribute to weight reduction. We also demonstrated activation of eNOS, which has the potential to improve diabetes-related vascular complications. Further studies are necessary to determine whether administration of oregano extract could aid in preventing the development of metabolic syndrome or in its treatment and amelioration of its complications.

ABBREVIATIONS USED

DMEM, Dulbecco's minimum essential medium; DMSO, dimethylsulfoxide; eNOS, endothelial nitric oxide synthase; DXS, 1-deoxy-D-xylulose 5-phosphate synthase; FCS, fetal calf serum; GST, glutathione-*S*-transferase; HUVECs, human um-

bilical vein endothelial cells; ITS, internal transcribed spacer; LBA, ligand binding assay; LBD, ligand binding domain; NO, nitric oxide; PPAR, peroxisome proliferator-activated receptor; SPPARγMs, selective PPARγ modulators; TR-FRET, time-resolved fluorescence resonance energy transfer.

LITERATURE CITED

(1) Alberti, G.; Zimmet, P.; Shaw, J.; Grundy, S. M. The IDF Consensus worldwide definition of the metabolic syndrome. http://www.idf.org/home/index.cfm?node=1429, 2006.

(2) Staels, B.; Fruchart, J. C. Therapeutic roles of peroxisome proliferator-activated receptor agonists. *Diabetes* **2005**, *54* (8), 2460–2470.

(3) Zhang, F.; Lavan, B. E.; Gregoire, F. M. Selective modulators of PPAR-γ activity: Molecular aspects related to obesity and side-effects. *PPAR Res.* **2007**.

(4) Rieusset, J.; Touri, F.; Michalik, L.; Escher, P.; Desvergne, B.; Niesor, E.; Wahli, W. A new selective peroxisome proliferator-activated receptor γ antagonist with antiobesity and antidiabetic activity. *Mol. Endocrinol.* **2002**, *16*, 2628–2644.

(5) Reilly, S. M.; Lee, C. H. PPARδ as a therapeutic target in metabolic disease. *FEBS Lett.* **2008**, *582* (1), 26–31.

(6) Yetik-Anacak, G.; Catravas, J. D. Nitric oxide and the endothelium: History and impact on cardiovascular disease. *Vasc. Pharmacol.* **2006**, *45*, 268–276.

(7) McCue, P. P.; Shetty, K. Inhibitory effects of rosmarinic acid extracts on porcine pancreatic amylase in vitro. *Asia Pac. J. Clin. Nutr.* **2004**, *13* (1), 101–106.

(8) Kim, J.-S.; Kwon, C.-S.; Son, K. H. Inhibition of α-glucosidase and amylase by luteolin, a flavonoid. *Biosci,. Biotechnol., Biochem.* **2000**, *64*, 2458–2461.

(9) Kwon, Y. I.; Vattem, D. A.; Shetty, K. Evaluation of clonal herbs of *Lamiaceae* species for management of diabetes and hypertension. *Asia Pac. J. Clin. Nutr.* **2006**, *15* (1), 107–118.

(10) Koga, K.; Shibata, H.; Yoshino, K.; Nomoto, K. Effects of 50% ethanol extract from rosemary (*Rosmarinus officinalis*) on α-glucosidase inhibitory activity and the elevation of plasma glucose level in rats, and its active compound. *J. Food Sci.* **2006**, *71*, S507–S512.

(11) Valentova, K.; Nhu, T. T.; Moncion, A.; De Waziers, I.; Ulrichova, J. Induction of glucokinase mRNA by dietary phenolic compounds in rat liver cells in vitro. *J. Agric. Food Chem.* **2007**, *55* (19), 7726–7731.

(12) Kang, D. G.; Oh, H.; Chung, H. T.; Lee, H. S. Inhibition of angiotensin converting enzyme by lithospermic acid B isolated from radix *Salviae miltiorrhiza* bunge. *Phytother. Res.* **2003**, *17* (8), 917–920.

(13) Ietswaart, J. *A Taxonomic Revision of the Genus Origanum (Labiatae)*; Leiden Botanical Series 4; Leiden University Press: The Hague, 1980.

(14) Doyle, J.; Doyle, J. Isolation of plant DNA from fresh tissue. *Focus* **1990**, *12*, 13–15.

(15) White, T.; Bruns, T.; Lee, S.; Taylor, J. Amplification and direct sequencing of fungal ribosomal RNA genes for phylogenetics. In *PCR Protocols: A Guide to Methods and Applications*; Innis, M., Gelfand, D., Sninsky, J., White, T., Eds.; Academic Press: San Diego, CA, 1990; Vol. 31, pp 315−322.

(16) Downie, S. R.; Katz-Downie, D. S. A molecular phylogeny of apiaceae subfamily apioideae: Evidence from nuclear ribosomal DNA internal transcribed spacer sequences. *Am. J. Bot.* **1996**, *83* (2), 234–251.

(17) Lukas, B.; Samuel, R.; Novak, J. Phylogenetic relationships in *Origanum* L. (Lamiaceae) based on ITS and DXS sequence data. Unpublished.

(18) Soltis, D.; Kuzzof, R. K. Discordance between nuclear and chloroplast phylogenies in the Heuchera Group (Saxifragaceae). *Evolution* **1995**, *49* (4), 727–742.

(19) Tamura, K.; Dudley, J.; Nei, M.; Kumar, S. MEGA4: Molecular Evolutionary Genetics Analysis (MEGA) software version 4.0. *Mol. Biol. Evol.* **2007**, *24* (8), 1596–1599.

(20) Staels, B.; Koenig, W.; Habib, A.; Merval, R.; Lebret, M.; Torra, I. P.; Delerive, P.; Fadel, A.; Chinetti, G.; Fruchart, J. C.; Najib, J.; Maclouf, J.; Tedgui, A. Activation of human aortic smooth-muscle cells is inhibited by PPARα but not by PPARγ activators. *Nature* **1998**, *393* (6687), 790–793.

(21) Jungbauer, A.; Graumann, K. The logistic dose-response function: A robust fitting function for transition phenomena in life sciences. *J. Clin. Ligand Assoc.* **2001**, *24* (4), 270–274.

(22) Simoncini, T.; Apa, R.; Reis, F. M.; Miceli, F.; Stomati, M.; Driul, L.; Lanzone, A.; Genazzani, A. R.; Petraglia, F. Human umbilical vein endothelial cells: A new source and potential target for corticotropin-releasing factor. *J. Clin. Endocrinol. Metab.* **1999**, *84* (8), 2802–2806.

(23) Simoncini, T.; Genazzani, A. R. Raloxifene acutely stimulates nitric oxide release from human endothelial cells via an activation of endothelial nitric oxide synthase. *J. Clin. Endocrinol. Metab.* **2000**, *85* (8), 2966–2969.

(24) Mueller, M.; Jungbauer, A. Red clover extract—A putative source for simultaneous treatment of menopausal disorders and metabolic syndrome. *Menopause* **2008**, *15* (6), accepted for publication.

(25) Kintzios, S. Profile of the multifaceted prince of the herbs. In *Oregano: The Genera Origanum and Lippia*; Kintzios, S. E., Ed.; Taylor and Francis, London, New York, 2002; pp 67−108.

(26) Shan, B.; Cai, Y. Z.; Sun, M.; Corke, H. Antioxidant capacity of 26 spice extracts and characterization of their phenolic constituents. *J. Agric. Food Chem.* **2005**, *53* (20), 7749–7759.

(27) Exarchou, V.; Godejohann, M.; Van Beek, T. A.; Gerothanassis, I. P.; Vervoort, J. LC-UV-solid-phase extraction-NMR-MS combined with a cryogenic flow probe and its application to the identification of compounds present in Greek oregano. *Anal. Chem.* **2003**, *75* (22), 6288–6294.

(28) Ross, R. Atherosclerosis—An inflammatory disease. *N. Engl. J. Med.* **1999**, *340* (2), 115–126.

(29) Vedavanam, K.; Srijayanta, S.; O'Reilly, J.; Raman, A.; Wiseman, H. Antioxidant action and potential antidiabetic properties of an isoflavonoid-containing soyabean phytochemical extract (SPE). *Phytother. Res.* **1999**, *13* (7), 601–608.

(30) Lindberg, M.; Astrup, A. The role of glitazones in management of type 2 diabetes. A DREAM or a nightmare? *Obes. Rev.* **2007**, *8* (5), 381–384.

Received for review July 25, 2008. Revised manuscript received October 6, 2008. Accepted October 30, 2008.

JF802298W